EUROPEAN COMMISSION

Community research

CROCK

(Contract Number: 269658)

DELIVERABLE (D-N°:1.2)
Characterization of experimental material

Author(s): **KIT-INE**

Reporting period: e.g. 31/07/12 – 30/06/13

Date of issue of this report: **31.12.2012**

Start date of project: **01/01/11** Duration: 30 Months

CROCK

EURATOM

DISTRIBUTION LIST

Name	Number of copies	Comments
Mr. Christophe Davies (European Commission)	One electronic copy submitted via participant portal	
All consortium members and European Commission	One electronic copy available on the restricted area of the CROCK webportal	

Project co-funded by the European Commission under the Seventh Euratom Framework Programme for Nuclear Research &Training Activities (2007-2011)		
Dissemination Level		
PU	Public	X
RE	Restricted to a group specified by the partners of the CROCK project	
CO	Confidential, only for partners of the CROCK project	

Summary of the work performed:

The objectives were to characterize the new samples of fracture crystalline rock drill-cores from the Äspö URL, sampled and handled under anoxic conditions. The characterization of the material is documented in (Schäfer et al., 2012) and the effect of the material (crushed material sieved to different size fractions) concerning radionuclide uptake is studied in detail as documented in (Stage et al., 2012) with special focus in redox sensitive radionuclides as Tc, see (Totskiy et al., 2012) for details. The main focus on this deliverable is on the characterization of fractured drill cores. More precisely, detailed results are shown for one of three drill cores selected to be suitable for experimental and modeling tasks. All cores presented in the deliverable in hand will be (or already has been in case of one core) characterized by computed tomography (CT) to obtain geometrical information on the fracture. This dataset can be used directly in numerical codes to carry out computational fluid dynamics (CFD) simulations, conservative solute transport as well as reactive transport calculations for radionuclide migration for comparison to experimentally obtained data.

Fractured cores

In addition to above mentioned activities regarding batch sorption studies on crushed material, characterization of natural fractures for radionuclide core migration studies have been performed. Drill cores with natural fractures oriented parallel or sub-parallel to the core length axis have been selected and are presented below. All fractures characterized here were artificially opened during the drilling procedure due to shear forces.

Core#1.22

This core represents foliated granite (Äspö diorite) with an open fracture at an angle of ~20° to the longitudinal axis of the core (Figure 1). Its position is around 8.63 m -8.81 m away from the tunnel surface. It shows a reddish color which may be attributed to a hydrothermal alteration (so called red-stained rock) (Drake et al., 2008). The fracture surfaces are covered with red mineral phases, most probably due to a high Fe content formed during the alteration.

Figure 1: Core#1.22. a) Core as obtained during the drilling campaign under inert gas atmosphere. b) View of the fracture suture. c) Details on both fracture surfaces showing a coating of reddish mineral phases. d) Core as prepared before gluing into the Plexiglas cylinder.

Core# 1.24

This core stems from the same drill hole as Core# 1.22 9.26 m – 9.74 m away from the tunnel surface (Figure 2). The rock color is more greyish with some reddish parts. The core starts with a fracture with an angle of 20°running with the core axis from 9.26 m – 9.53 m. At 9.70 m a fracture starts which has been fragmented into smaller pieces during drilling. The fracture surfaces rims show reddish-yellowish colors which may be attributed again to Fe containing phases. The majority of the fracture surfaces show grey to black colors in contrast to the core #1.22. It seems that this core section has not been chemically and mineralogical altered by hydrothermal fluids as it has been the case for Core# 1.22. Regarding this differences, it will be interesting to examine the effect of the mineralogy on the radionuclide transport between these 2 cores.

Figure 2: Core#1.24. a) Core as obtained during the drilling campaign under inert gas atmosphere. b) View of the fracture suture. c) Details on both fracture surfaces. d) Core as prepared before gluing into the Plexiglas cylinder.

Core# 2.2

In Figure 3 the natural fracture of the drill core section #2.2 (0.53 m -0.97 m) from drill hole KA2370A-01 is shown before starting of the preparative work. All preparative steps described below have been performed in an Ar glovebox with < 1ppm O_2 to avoid oxidation. This core was chosen first to test the general applicability of the preparative procedure since it is located close to the tunnel surface and thus likely influenced by oxygen. A failure of the procedure would not have led to a loss of more scientific valuable core material located in anoxic zones (Cores#1.22&1.24). The core was cut in length to extract the fractured section for further preparation. Figure 4a shows the remaining two parts after cutting of the core also displaying both fracture surfaces

Figure 3: Drill core section #2.2 (0.53-0.97 m) from drill hole KA2370A-01 with a natural fracture.

Subsequently, both parts have been assembled together to obtain the original position as far as possible and fixed with tape and a bar clamp without applying excessive pressure (Figure 4b). Afterwards, the suture (outer rim) of the fracture was glued using high viscous Plexiglas glue. The glue process was done stepwise applying only very small amounts of glue in each step to avoid potential intrusion of the glue into the fracture itself. To achieve this, the part to be glued was always in a head first position. Several layers of glue have been applied to guaranty that the fracture rim is fully sealed. After finalization of the glue process the core was placed in a Plexiglas cylinder and the remaining void space between core and inner wall of the cylinder was filled up using the same glue as mentioned above. After drying of the glue, the upper and lower bottom of the core was sawed again and carefully polished by hand to obtain smooth surfaces before the top and bottom cap was glued onto the core (Figure 4c).

For characterization of the fracture the drill core was scanned using micro computed tomography (µCT) with a resolution of 16 µm. Figure 4d depicts a µCT slice where the fracture is clearly seen as a black irregular line running from the upper left to the lower right. Out of the µCT dataset a 3D digital model has been prepared using the software Mimics© and 3matic© (both Materialise, Belgium) by greyscale threshold segmentation of the dataset extracting only the connected void space (fracture).

The geometry of the fracture reconstructed by the µCT dataset is shown in Figure 5 for different orientations. It can be clearly seen, that the fracture possess heterogeneous, rough and slightly bended surfaces with several locations in the upper half of the fracture where both surfaces interconnect each other (asperities) meaning that the fracture is closed at this

points. A distribution of the aperture (opening width of the fracture) has been derived from the 3D model which is shown in Figure 6. It is obvious that the aperture is heterogeneously distributed due to the complex geometry of the natural fracture surfaces. As mentioned above the asperities represent locations where the aperture is not detectable by µCT (< 16µm). The highest aperture is 0.8093 mm (mid to high apertures are indicated in Figure 6 with yellow to red colors, respectively). A mean aperture 0.192 mm with a standard deviation of 0.0637 mm has been obtained (mid to low apertures are represented by yellow to green colors, respectively). The total fracture surface area was determined to be 0,004235 m^2 and the total volume of the fracture void space is 0.415 ml.

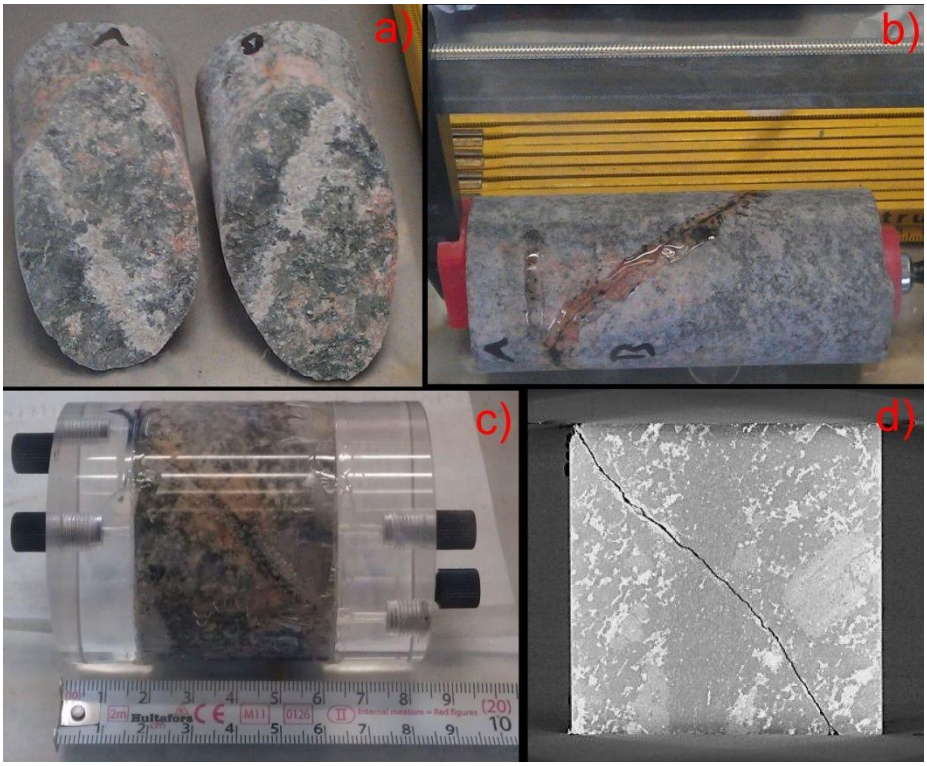

Figure 4: Core#2.2. a) Details on both fracture surfaces. b) Core as prepared before gluing into the Plexiglas cylinder. c) Core after preparation fitted with tubing ready for CT measurements and the migration experiments. d) CT slice of the core showing the open fracture (black line from bottom right to upper left).

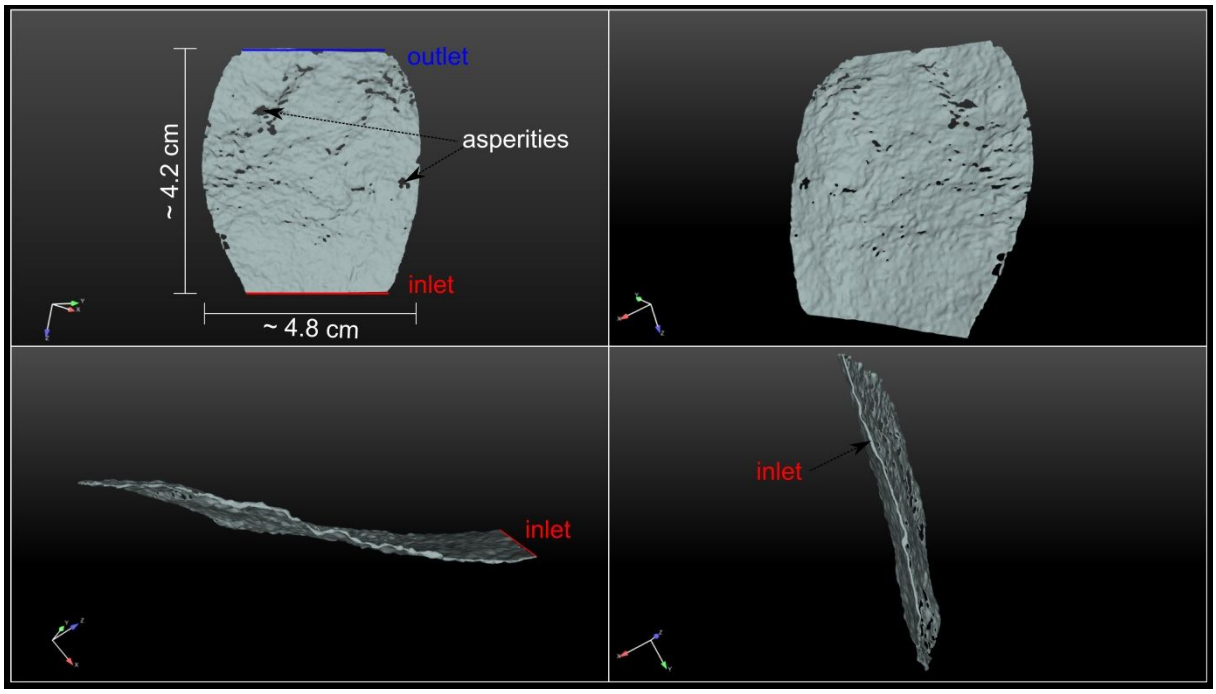

Figure 5: Different views of the rendered fracture geometry as obtained by the CT dataset. Notice the heterogeneous geometry and the various asperities.

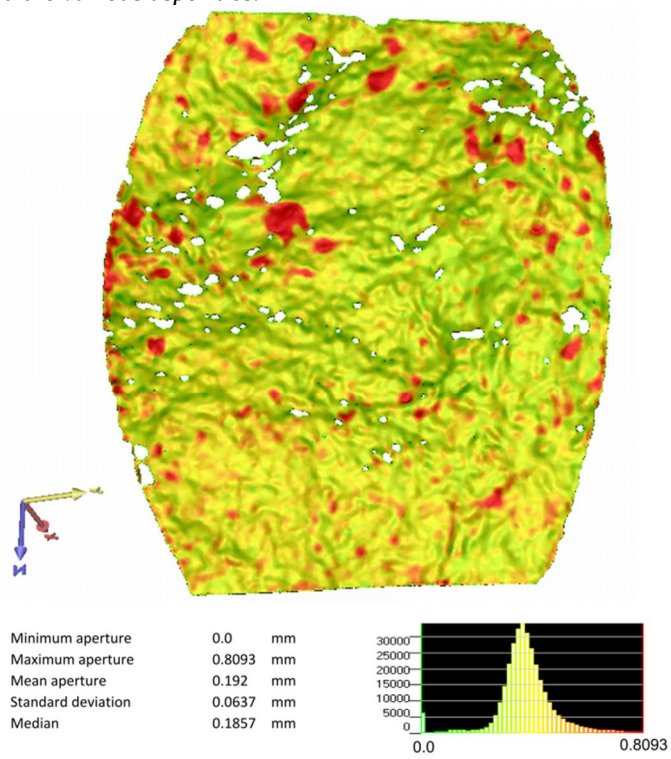

Figure 6: Aperture distribution of Core#2.2. Red color indicates high apertures, green color represents zero to low apertures. Notice the heterogeneous distribution of the aperture as function of the complex fracture geometry.

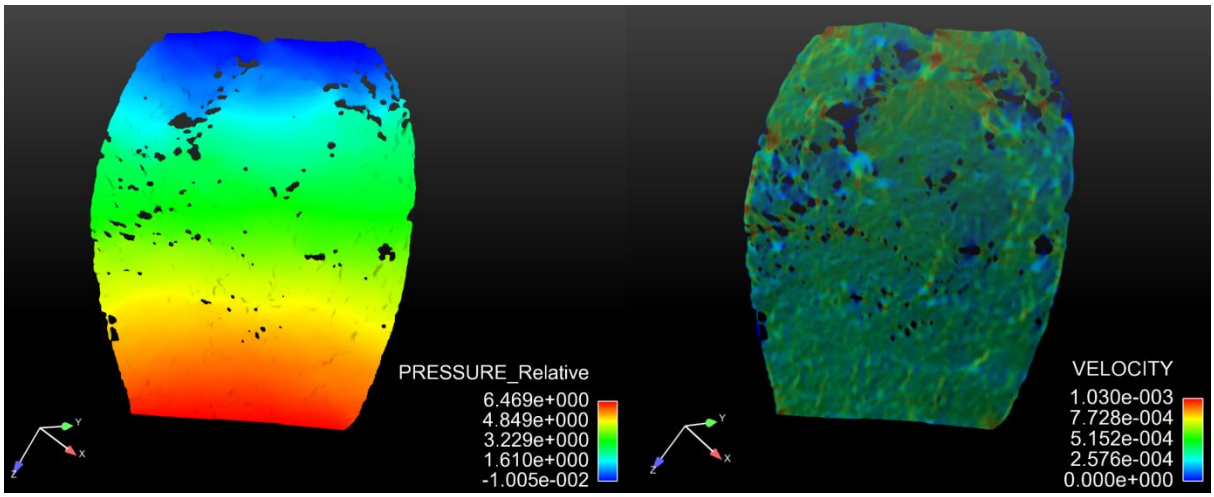

Figure 7: Left: Pressure distribution. Right: Volume plot of the velocity magnitude. Legend is rescaled to 1.03e-3 m/s for viewing reasons. The maximum velocity magnitude is 3.4e-3 m/s.

Further pre-processing of the dataset applying the meshing tool ICEMCFD© (Ansys) resulted in a 3D numerical mesh (~ 5 Mio. triangular and tetrahedral elements in total) suitable for Navier-Stokes based flow simulations with the computational fluid dynamics solver Fluent© (Ansys). Results of these simulations are presented in Figure 7 which shows the pressure distribution and a volume plot of the velocity field. The complex flow velocity distribution results from the heterogeneous fracture geometry and aperture distribution. Especially, the asperities lead to channeling of the flow into preferred regions of the fracture. This can be seen in Figure 8 where a particle traces plot is depicted. The virtual particles travel on the streamlines and are not influenced by other forces like e.g. diffusion but advection only. It can be clearly seen that the particles are strongly dispersed by the flow velocity distribution governed by the fracture geometry. The evolution of fingering of the flow and in consequence of several flow "highways" is visible. That is, the natural fracture geometry leads to a dispersion of a solute or particles only due to the fracture geometry. This observation is corroborated by similar studies on other drill cores from Äspö (Huber et al., 2012). First conservative solute transport simulations using the code FLUENT (ANSYS) are carried out at the moment.

First conservative tracers test have been carried out on this drill core. Tritium has been applied in the experiments as nonreactive solute. As an example, a breakthrough curve (BTC) is shown in Figure 9. The BTC obeys a sharp rising edge followed by a pronounced late time arrival of the solute (tailing). After ~ 110 min the flow was stopped for ~ 3 d and started again, now showing a different slope in the tailing of the curve. This may be attributed to a different process, most likely matrix diffusion. A detailed analysis of the results and further experiments applying also a cocktail of radioactive tracers (e.g. ^{95m}Tc, ^{152}Eu, ^{233}U, ^{137}Cs) are carried out at the moment.

Permeability (m^2) and kf- values (m/s) were measured in the experimental setup via pressure sensors of 0.1 mbar resolution and syringe pump establishing a constant flow rate.

Measurements under three different gradients revealed permeability of $4.0\text{-}4.7 \cdot 10^{-14}$ m^2 and kf-values of $3.0\text{-}3.5 \cdot 10^{-10}$ m/s, respectively.

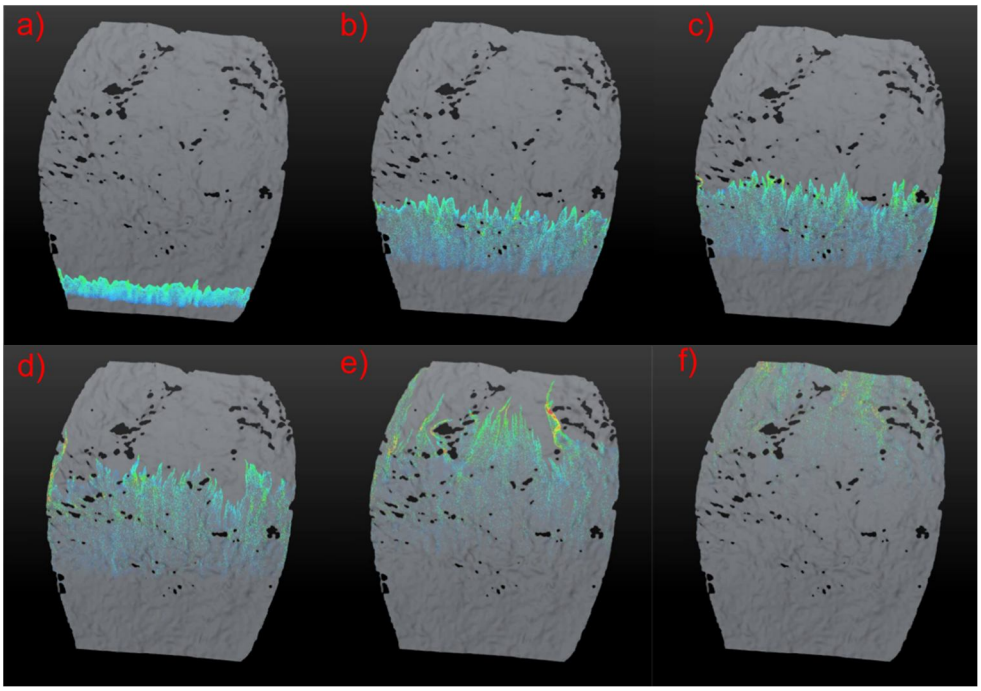

Figure 8: Particle traces plots of the flow field. Notice the spreading of the virtual particles due to the complex fracture geometry. The color of the particles are representative of the velocity magnitude.

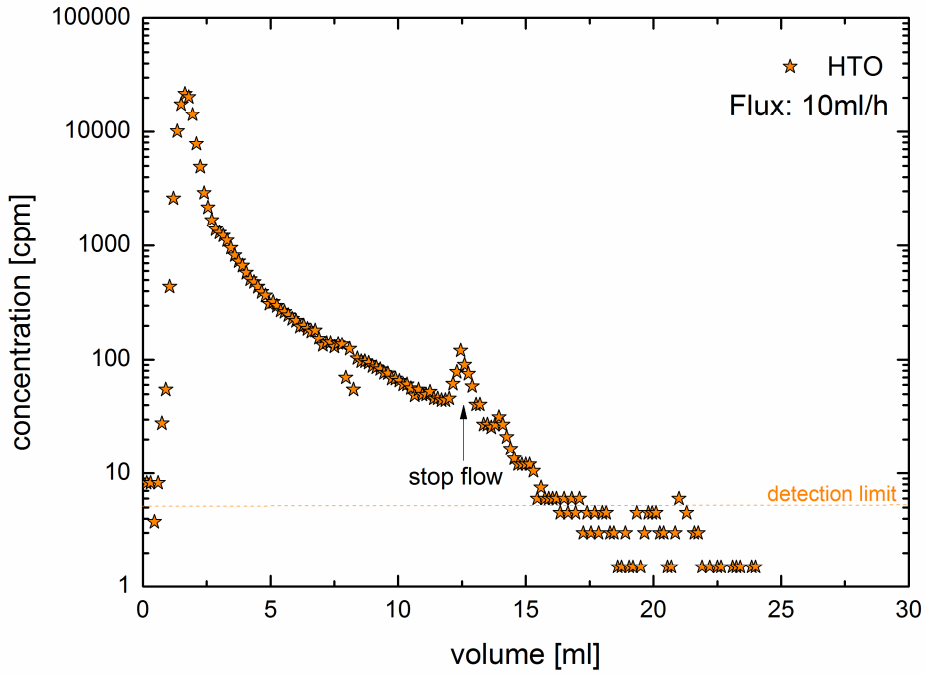

Figure 9: Experimental HTO breakthrough curve.

References

Drake, H., Tullborg, E.-L. and Annersten, H., 2008. Red-staining of the wall rock and its influence on the reducing capacity around water conducting fractures. Applied Geochemistry, 23(7): 1898-1920.

Huber, F. et al., 2012. Natural micro-scale heterogeneity induced solute and nanoparticle retardation in fractured crystalline rock. Journal of Contaminant Hydrology, 133(0): 40-52.

Schäfer, T., Stage, E., Büchner, S., Huber, F. and Drake, H., 2012. Characterization of new crystalline material for investigations within CP CROCK. In: T. Rabung, J. Molinero, D. Garcia and V. Montoya (Editors), 1st Workshop Proceedings of the Collaborative Project "Crystalline Rock Retention Processes" (7th EC CP CROCK), KIT Scientific Reports 7629. Karlsruhe Institute of Technology (KIT), Stockholm (Sweden), pp. 63-72.

Stage, E., Huber, F., Heck, S. and Schäfer, T., 2012. Sorption/Desorption of ^{137}Cs(I), ^{152}Eu(III) and ^{233}U(VI) onto new CROCK derived Äspö diorite - a batch type study. In: T. Rabung, J. Molinero, D. Garcia and V. Montoya (Editors), 1st Workshop Proceedings of the Collaborative Project "Crystalline Rock Retention Processes" (7th EC CP CROCK), KIT Scientific Reports 7629. Karlsruhe Institute of Technology (KIT), Stockholm (Sweden), pp. 51-62.

Totskiy, Y., Geckeis, H. and Schäfer, T., 2012. Sorption of Tc(VII) on Äspö diorite (ÄD). In: T. Rabung, J. Molinero, D. Garcia and V. Montoya (Editors), 1st Workshop Proceedings of the Collaborative Project "Crystalline Rock Retention Processes" (7th EC CP CROCK), KIT Scientific Reports 7629. Karlsruhe Institute of Technology (KIT), Stockholm (Sweden), pp. 97-106.